LOW COMPLEXITY SPACE-FREQUENCY RAKE RECEIVERS FOR WCDMA

Christopher Brunner,[1, 2] Martin Haardt,[*] [1] and Josef A. Nossek [2]

1. Siemens AG, ICN CA CTO 71
Hofmannstr. 51, D-81359 Munich, Germany
Phone / Fax: +49 (89) 722-29480 / -44958
E-Mail: Martin.Haardt@icn.siemens.de

2. Institute for Network Theory and Circuit Design
Munich Univ. of Technology, D-80290 Munich, Germany
Phone / Fax: +49 (89) 289-28511 / -28504
E-Mail: Christopher.Brunner@ei.tum.de

ABSTRACT

Adaptive space-frequency rake receivers use diversity combining and multi-user interference suppression to obtain a considerable increase in performance in DS-CDMA systems such as WCDMA. The main advantages of operation in the space-frequency domain include a reduced computational complexity and an improved noise suppression. To this end, the signal-plus-interference-and-noise (SIN) and the interference-plus-noise (IN) space-frequency covariance matrices are required. The optimum weight vector for symbol decisions is the "largest" generalized eigenvector of the resulting matrix pencil. If we decouple spatial and frequency processing with respect to interfering users, the IN space-frequency covariance matrix can be approximated by the Kronecker product of the frequency and the spatial covariance matrix. Then this IN covariance matrix is estimated by using the outputs of the antenna elements before correlation and the output of the conventional rake fingers of the antenna elements may be utilized to approximate the SIN covariance matrix. Thus, the required correlations are reduced to the number of rake fingers. Moreover, the computational complexity which is required to estimate the optimum weight vector may be reduced significantly.

1. INTRODUCTION

Adaptive antennas exploit the inherent spatial diversity of the mobile radio channel and are, therefore, seen as an important technology to meet the high spectral efficiency and quality requirements of third generation mobile radio systems. The proposed concepts for the third generation [4] allow an easy and flexible implementation of new and more sophisticated services. Recently, ETSI SMG selected the TD-CDMA concept as the radio access scheme for time-division duplex systems and the WCDMA concept for frequency-division duplex systems. This solution has been contributed to the International Telecommunication Union - as the European proposal for IMT-2000 transmission technology.

The main advantage of the conventional space-time rake [5] for single-user data detection is its simplicity. However, since co-channel interferers are not taken into account, the conventional space-time rake is not near-far resistent. A space-frequency rake [6, 1, 2] based on space-frequency covariance matrices combines each multipath across space and frequency, performs multi-user interference suppression in addition to diversity combining, and, therefore, mitigates the stringent power control requirements common to DS-CDMA systems. Hence, a direct capacity increase is achieved by transmitting more codes with lower spreading factors. Due to the reduced transmission rate for uplink power control due to mitigated power control requirements, the downlink capacity for data transmission is also increased.

In this paper, we examine a low-complexity space-frequency rake receiver which is characterized by decoupled spatial and frequency processing with respect to interfering users and spatial interference suppression. In this case, the IN space and frequency covariance matrices can be estimated very efficiently by using the outputs of the antenna elements before correlation. The SIN space-frequency covariance matrix is approximated with the outputs of the rake fingers of a conventional rake receiver. Thus, there are only as many correlations required as rake fingers exist, which is a significant reduction compared to the space-frequency rake described in [2]. Moreover, the optimum weight vector can be estimated very efficiently due to the structure of the approximated IN space-frequency covariance matrix. Notice, however, that the performance of the low-complexity space-frequency rake is degraded, since joint space-frequency processing is not done with respect to interfering users in constrast to, e.g., the space-frequency rake described in [2].

This paper is organized as follows. Taking into account the uplink channel structure of WCDMA, which is described in Section 2, we explain the estimation of the SIN space-frequency covariance matrix along with the IN space-frequency covariance matrix and the estimation of the optimum weight vector in Section 3. The conventional space-time rake receiver, the space-frequency rake receiver, and the low-complexity space-frequency rake receiver are explained in Section 4. Section 5 compares the different rake receivers by means of Monte-Carlo simulations with respect to performance and computational complexity. In the sequel, adaptive antennas are only assumed at base stations. The space-frequency rake, however, also applies to mobiles with adaptive antennas.

2. WCDMA UPLINK CHANNEL STRUCTURE

WCDMA has two types of dedicated physical channels on the uplink (and the downlink), the PCCH and the PDCH. In case of low and medium data rates, one connection consists of one PCCH and one PDCH [4]. The PDCH baseband signal of the user of interest may be expressed as $s_D(t) = \sum_{\ell=-\infty}^{\infty} b_D^{(\ell)}\, z_D(t-\ell T_D)$, $\quad z_D(t) = \sum_{m=1}^{n_D} d_D^{(m)}\, p(t-mT_c)$. The chip rate in WCDMA is $1/T_c = 4.096$ Mchips/s.

0-7803-5639-X/99/$10.00 ©1999 IEEE.

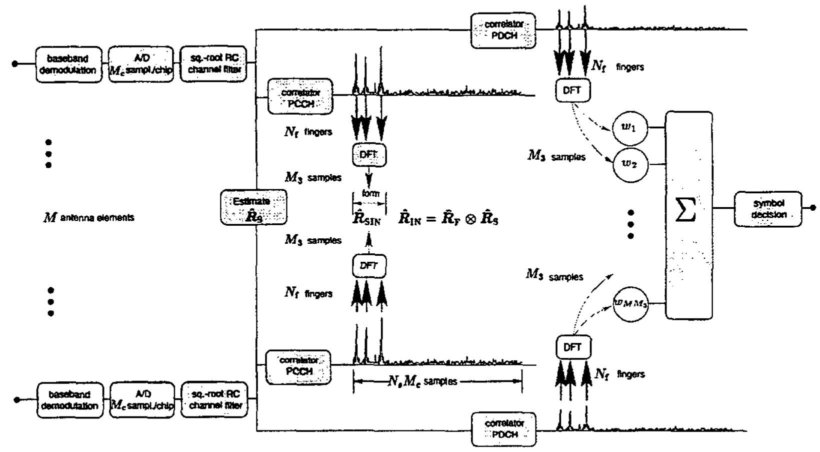

Figure 1: Structure of the low-complexity space-frequency rake receiver: The N_P pilot symbols at the beginning of each PCCH slot are used to generate the space-frequency covariance matrices $\hat{R}_{SIN}$ and $\hat{R}_{IN}$. The "largest" generalized eigenvector w, which is the optimum weight vector, is applied to the PCCH and PDCH to obtain the remaining control symbols and the data symbols, respectively.

Moreover, the spreading sequence of the PDCH, $z_D(t)$, is of length $T_D = n_D T_c$ and is composed of n_D chips $d_D^{(m)} \in \{-1, 1\}, 1 \leq m \leq n_D$. The symbols, $b_D^{(\ell)} \in \{-1, 1\}$, are BPSK modulated. WCDMA uses a chip waveform, $p(t) \in \mathbb{R}$, characterized by a square-root raised cosine spectrum with a rolloff factor of $\alpha = 0.22$.

The PCCH baseband signal, $s_C(t)$, can be expressed in the same way. A combination of code and IQ multiplexing is used on the uplink, where the PDCH and the PCCH are spread by different spreading codes [4] and mapped to the I and Q branches, respectively, according to $s(t) = s_D(t) + \mathrm{j} \cdot s_C(t)$. Next, the complex I + jQ signal is either scrambled by a complex short code (256 chips) or by a complex long code (40960 chips) [4]. For simplicity, we do not include scrambling in our notation.

3. GENERATION OF THE COVARIANCE MATRICES

We assume that the receiver is synchronized to the beginning of a slot. The searcher of a conventional rake [5] is applied to the correlator output of each antenna to estimate N_f correlation peaks per antenna element. The corresponding correlator sequence is given by $c_P(nT_1) = \sum_{\ell=0}^{N_P-1} b_C^{(\ell)} z_C(nT_1 - \ell T_C)$, where N_P denotes the number of pilot symbols which are transmitted at the beginning of each PCCH slot. Recall that complex scrambling is required but not considered in our notation. Each finger is characterized by its delay $g_{m,n} T_1$ and complex amplitude $w_{m,n}$, where $1 \leq n \leq N_f$ and $1 \leq m \leq M$ denote the rake finger and the antenna element, respectively. Let $\mathcal{X}_P$ contain the correlation outputs corresponding to the rake fingers according to

$$\mathcal{X}_P|_{(m, g_{m,n})} = w_{m,n} \quad \forall \quad m, n, \tag{1}$$

where $\mathcal{X}_P^{(\ell)}|_{(y,x)}$ denotes the y-th element in the x-th column of the matrix $\mathcal{X}_P$. Each row and each column of $\mathcal{X}_P \in \mathbb{C}^{M \times N_w}$ corresponds to an antenna element and a delay, respectively. The length of the delay spread of the user of interest in samples is denoted by $N_w = M_c \frac{\tau_{\max}}{T_c}$, where $M_c = T_C/T_1$ is the oversamping factor. Next, a space-frequency transformation is performed by post-multiplying the selected correlation output with the N_w-point DFT matrix W_T according to

$$y_P = \mathrm{vec}\{\mathcal{X}_P W_T\} \in \mathbb{C}^{M_3 M}. \tag{2}$$

The vec-operator maps an $m \times n$ matrix into an mn-dimensional column vector by stacking the columns of the matrix. Each column of W_T is of the form $w_\ell = \begin{bmatrix} 1 & e^{-\mathrm{j}\ell\omega_0} & e^{-\mathrm{j}2\ell\omega_0} & \ldots & e^{-\mathrm{j}(N_w-1)\ell\omega_0} \end{bmatrix}^T$. Here, the columns of W_T compute $M_3 \leq N_w$ frequency bins centered at DC according to $W_T = \begin{bmatrix} w_{N_w-(M_3-1)/2} & \cdots & w_0 & \cdots & w_{(M_3-1)/2} \end{bmatrix}$, where we have invoked the wrap-around property of the DFT matrix. Assuming that the channel stays approximately constant for at least one slot, the space-frequency SIN covariance matrix

$$\hat{R}_{SIN} = y_P \cdot y_P^H \tag{3}$$

multipath channel	user of interest	interferer # 1	interferer # 2	interferer # 3
wavefront # 1	(+35.4°, 30.9, 0.57)	(-81.6°, 00.0, 1.34)	(-62.0°, 12.6, 0.56)	(+46.9°, 19.4, 1.00)
wavefront # 2	(+13.3°, 08.5, 1.71)	(-82.9°, 03.7, 0.75)	(+74.5°, 32.6, 1.03)	(-59.5°, 13.7, 0.73)
wavefront # 3	(-20.4°, 19.4, 0.66)	(-71.5°, 09.3, 0.66)	(+59.6°, 30.1, 0.71)	(-88.3°, 09.9, 0.57)
wavefront # 4	(-26.4°, 35.4, 1.52)	(+71.4°, 04.3, 0.98)	(-31.1°, 20.4, 1.04)	(+82.9°, 39.5, 0.73)

Table 1: The user of interest and three interferers are modeled by a simple four-ray multipath channel. Each ray is characterized by its angle of arrival with respect to the boresight of the base station ULA in degrees, by its delay in chips, and by its attenuation - the table contains the absolute values of the complex attenuations.

is estimated by using only one space-frequency snapshot that contains the multipaths of the user of interest, cf. Figure 1. If we decouple spatial and frequency processing with respect to the interferers, the IN space-frequency covariance matrix can be approximated by the Kronecker product of the frequency and the spatial covariance matrix according to

$$\hat{\boldsymbol{R}}_{\mathrm{IN}} = \hat{\boldsymbol{R}}_{\mathrm{F}} \otimes \hat{\boldsymbol{R}}_{\mathrm{S}}, \tag{4}$$

where $\hat{\boldsymbol{R}}_{\mathrm{F}}$ and $\hat{\boldsymbol{R}}_{\mathrm{S}}$ denote estimates of the frequency and the spatial covariance matrix, respectively. Moreover, $\otimes$ denotes the Kronecker product. Next, space-frequency interference suppression is reduced to spatial interference suppression by approximating the frequency covariance matrix with an identity matrix of dimension $M_3 \times M_3$. To this end, the noisy space-frequency bins must be omitted. The spatial covariance matrix can be estimated at the antenna element outputs according to $\hat{\boldsymbol{R}}_{\mathrm{S}} = \frac{1}{N_s M_c} \sum_{n=1}^{N_s M_c} \boldsymbol{x}(nT_{\mathrm{I}}) \cdot \boldsymbol{x}^H(nT_{\mathrm{I}})$, where $\boldsymbol{x}(nT_{\mathrm{I}})$ denotes the samples at the antenna array at nT_{I}.

4. RAKE RECEIVER STRUCTURES

We assume that the receiver is synchronized to the beginning of the ℓth bit in the PDCH slot.

4.1. Conventional Space-Time Rake Receiver

The correlator sequence is defined according to $c_{\mathrm{D}}(nT_{\mathrm{I}}) = z_{\mathrm{D}}(nT_{\mathrm{I}})$, where z_{D} denotes the spreading code of the PDCH channel. Then the decision variables are obtained by maximum ratio combining

$$\hat{b}_{\mathrm{D}}^{(\ell)} = \sum_{m=1}^{M} \sum_{n=1}^{N_{\mathrm{f}}} w_{m,n}^{H} \cdot \mathcal{X}_{\mathrm{D}}^{(\ell)}|_{(m, g_{m,n})} = \mathrm{vec}\left\{\mathcal{X}_{\mathrm{P}}\right\}^{H} \mathrm{vec}\left\{\mathcal{X}_{\mathrm{D}}^{(\ell)}\right\}, \tag{5}$$

where $\mathcal{X}_{\mathrm{D}}^{(\ell)}$ contains the correlation outputs corresponding to the delays of the rake fingers and the ℓth bit of the PDCH slot.

4.2. Low-Complexity Space-Frequency Rake Receiver

By estimating the space-frequency IN covariance matrix $\boldsymbol{R}_{\mathrm{IN}}$ in addition to the space-frequency SIN covariance matrix $\boldsymbol{R}_{\mathrm{SIN}}$, the signal to interference and noise ratio

$$\mathrm{SINR} = \max_{\boldsymbol{w}} \frac{\boldsymbol{w}^H \boldsymbol{R}_{\mathrm{S}} \boldsymbol{w}}{\boldsymbol{w}^H \boldsymbol{R}_{\mathrm{IN}} \boldsymbol{w}} = \max_{\boldsymbol{w}} \frac{\boldsymbol{w}^H \boldsymbol{R}_{\mathrm{SIN}} \boldsymbol{w}}{\boldsymbol{w}^H \boldsymbol{R}_{\mathrm{IN}} \boldsymbol{w}} - 1 \tag{6}$$

can be maximized. The weight vector $\boldsymbol{w}$ yielding the optimum SINR for symbol decisions, cf. Section 4.2, is the "largest" generalized eigenvector of the $L_S M_3 \times L_S M_3$ matrix pencil $\{\hat{\boldsymbol{R}}_{\mathrm{SIN}}, \hat{\boldsymbol{R}}_{\mathrm{IN}}\}$. By transforming the covariance matrices into the space-frequency domain, noisy space-frequency bins with low signal power can be omitted, thus reducing the size of the covariance matrices and the computational complexity of (6). Moreover, an improved noise suppression is attained. Note that the space-frequency SIN covariance matrix $\hat{\boldsymbol{R}}_{\mathrm{SIN}}$ estimated in (3) has rank one. Therefore, a scaled version of $\boldsymbol{w}$ is given by $\hat{\boldsymbol{R}}_{\mathrm{IN}} \boldsymbol{w}' = \boldsymbol{y}_{\mathrm{P}}$. In [2], a Cholesky factorization [3] of $\hat{\boldsymbol{R}}_{\mathrm{IN}}$ was performed in order to obtain $\boldsymbol{w}'$ by solving two triagonal systems, exploiting that $\hat{\boldsymbol{R}}_{\mathrm{IN}}$ is positive definite and symmetric. Due to the block diagonal structure of $\hat{\boldsymbol{R}}_{\mathrm{IN}}$, cf. (4), it is sufficient to invert only one (positive definite and symmetric) block of dimension $M \times M$ instead of $\hat{\boldsymbol{R}}_{\mathrm{IN}}$ of dimension $MM_3 \times MM_3$. Each block is equal to the spatial covariance matrix $\hat{\boldsymbol{R}}_{\mathrm{S}}$. The snapshot corresponding to the ℓth bit of the PDCH slot is obtained according to (2) as $\boldsymbol{y}_{\mathrm{D}}^{(\ell)} = \mathrm{vec}\{\mathcal{X}_{\mathrm{D}}^{(\ell)} \boldsymbol{W}_{\mathrm{T}}\}$ for operation in the space-frequency domain, where $\mathcal{X}_{\mathrm{D}}^{(\ell)}$ is obtained as in Section 4.1. With the optimum weight vector $\boldsymbol{w}$ defined in (6), the optimum decision statistic [6] may then be computed as

$$\hat{b}_{\mathrm{D}}^{(\ell)} = \boldsymbol{w}^H \cdot \boldsymbol{y}_{\mathrm{D}}^{(\ell)}. \tag{7}$$

5. SIMULATION RESULTS

A simple four-ray multipath channel is assumed for the user of interest as well as for three interfering users. The (time-invariant) channel parameters are given in Table 1. Weaker interfering users are modeled by adding white Gaussian noise to the channel. We assume a maximum delay spread of $\tau_{\max} \approx 10\mu s$ which corresponds to 40 chips. Adjacent sensors of the base station ULA are separated by half a wavelength. Moreover, long scrambling codes were used. Further simulation parameters are given in Figure 2.

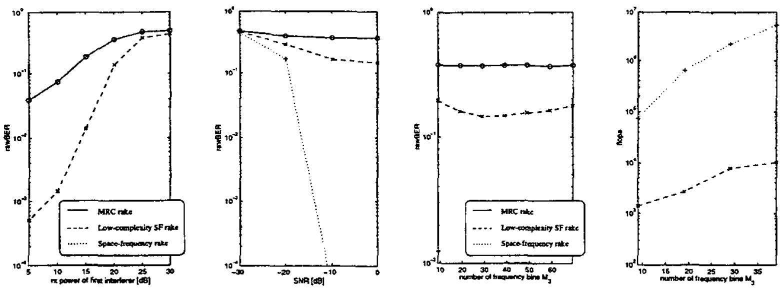

(a) (b) (c) (d)

Figure 2: The conventional space-time rake, the space-frequency rake, and the low-complexity space-frequency rake, are denoted by 'o', '+', and 'x', respectively. The performance criterion is the raw bit error ratio (BER) averaged over 1000 slots. Figure (a) shows the performance as a function of the power of the first interfering user at the receiver in relation to the power of the user of interest in dB. The space-frequency rake has a BER of less than 10^{-4}. Figure (b) indicates the influence of noise in relation to the power of the user of interest in dB. The performance as a function of the number of frequency bins M_3 is shown in Figure (c). If not stated otherwise, the following parameters hold: $M_c = 2, N_\omega = 79, M_3 = 29, M = 4, \mathrm{SNR} = -10$ dB, $\mathrm{SIR}_1 = -20$ dB, $\mathrm{SIR}_2 = -10$ dB, $\mathrm{SIR}_3 = -15$ dB, $n_D = 128, n_C = 256, N_P = 6, N_f = 3$. Figure (d) shows the computational complexity which is required to estimate the optimum weight vector in flops as a function of the considered space-frequency bins for the space-frequency rake and the low-complexity space-frequency rake.

In Figure 2 (a), the power of the first of three interfering users at the receiver is varied between 5 dB and 30 dB with respect to the power of the signal of interest. The power of the second and third interferers equals $\mathrm{SIR}_2 = -10$ dB and $\mathrm{SIR}_3 = -15$ dB, respectively. In contrast to the conventional space-time rake, the space-frequency rake is near-far resistent. It is able to suppress the interferers over the complete range and, therefore, has a BER of less than 10^{-4}. The performance of the low-complexity space-frequency rake lies between both previous schemes. If the first interferer is weak, spatial interference suppression alone is able to achieve near-far resistance. However, as the first interferer becomes stronger, the degrees of freedom offered by spatial interference suppression alone are not sufficient. Figure 2 (b) shows the influence of noise in relation to the power of the user of interest in dB. Note that both space-frequency rakes only use $M_3 = 29$ of $N_\omega = 79$ available space-frequency bins. The frequency bins centered around DC have more signal energy. Therefore, weaker frequency bins can be omitted. The spectrum of the raised-cosine signal determines the strong and the weak frequency bins. Due to noise effects, the performance degrades if the weak frequency bins are considered, cf. Figure 2 (c). Figure 2 (d) shows the computational complexity which is required to estimate the optimum weight vector in flops as a function of the considered space-frequency bins for the space-frequency rake and the low-complexity space-frequency rake. The computational complexity required by the low-complexity space-frequency rake is more than two magnitudes lower than the computational complexity required by the space-frequency rake of [2] and increases linearly with respect to the number of space-frequency bins. Note that the optimum weight vector must be estimated each slot ($T_{\mathrm{slot}} = 0.625$ms).

6. CONCLUDING REMARKS

In this paper, we have presented a low-complexity space-frequency rake receiver for data detection with adaptive antennas in WCDMA. Simulation results show that there is an excellent tradeoff in terms of complexity and performance when comparing the low-complexity space-frequency rake with the conventional MRC space-time rake and the space-frequency rake as described in [2]. The covariance matrices required for near-far resistant multi-user interference suppression are estimated utilizing the same number of correlations as required by a MRC space-time rake receiver. Moreover, the computational complexity required to estimate the optimum weight vector is reduced significantly. Of course, the degrees of freedom available for interference suppression are limited to spatial interference suppression and, therefore, the low-complexity space-frequency rake performs superior to the MRC rake but inferior to the space-frequency rake.

7. REFERENCES

[1] C. Brunner, M. Haardt, and J. A. Nossek, "2-D rake receiver in the space-frequency domain for the uplink of WCDMA", in *Proc. 6th IEEE International Workshop on Intelligent Signal Processing and Communication Systems, (ISPACS '98)*, vol. 2, pp. 551-555, Melbourne, Australia, Nov. 1998.

[2] C. Brunner, M. Haardt, and J. A. Nossek, "Adaptive space-frequency rake receivers for WCDMA", in *Proc. IEEE Int. Conf. Acoust., Speech, Signal Processing*, Phoenix, Arizona, Mar. 1999, accepted for publication.

[3] G. H. Golub and C. F. van Loan, *Matrix Computations*, Johns Hopkins University Press, Baltimore, MD, 2nd edition, 1989.

[4] E. Nikula, A. Toskala, E. Dahlman, L. Girard, and A. Klein, "FRAMES Multiple Access for UMTS and IMT-2000", *IEEE Pers. Comm. Mag.*, Apr. 1998.

[5] J. G. Proakis, *Digital Communications*, McGraw-Hill, New York, NY, 2nd edition, 1989.

[6] M. D. Zoltowski, J. Ramos, C. Chatterjee, and V. Roychowdhury, "Blind adaptive 2D rake receiver for DS-CDMA based on space-frequency MVDR processing", *IEEE Trans. Signal Processing*, June 1996, submitted for publication.